Rev. Roum. Sci. Techn.– Électrotechn. et Énerg.
Vol. **62**, *4*, pp. 431–435, Bucarest, 2017

CONSIDERATIONS ON A GEOTHERMAL ELECTRIC POWER GENERATOR BASED ON ORGANIC RANKINE CYCLE AS A PART OF A SMART-GRID

MARIUS OVIDIU NEAMTU[1], MUGUR BALAN[2], DORIN PETREUS[2], TEODOR LEUCA[1], NISTOR DANIEL TRIP[1]

Key words: Geothermal power, Organic Rankine cycle, Thermal generator.

Taking into account the new trends in the renewable energy applications and the availability of the geothermal water resources in Oradea, the authors present in this paper a study regarding the possibility to integrate a geothermal generator into a smart-grid. The operation of the geothermal generator is modelled and simulated for a large domain of variation of the thermal agent to cover all available geothermal global parameters. The importance of the study results from the actual trend in the development of the smart-grids that comprises different kind of renewable sources to obtain a higher energetic autonomy and to offer a more flexible use of the electrical energy.

1. INTRODUCTION

It is obvious that the use of the solar and wind energies are more and more used both in public and private applications, such as [1–3] and so on. Despite of this fact, these energies could be predicted with a good approximation but they are not completely available or they encounter a high variation that depends on the stochastic meteorological conditions. Such problems can be solved using auxiliary expensive electric power storage units [4, 5]. An example of a clean power plant operating with hydrogen based on the Rankine cycle is presented in [6]. In areas with geothermal potential, the storage of the energy obtained from renewable energy sources can be changed with a thermal generator that uses geothermal waters to produce electricity. The geothermal energy sources are more predictable, offering a quasi-constant level of power energy during the whole year period [7]. An evaluation of the geothermal exploitation systems is described in [8].

The operation of the geothermal generators uses different types of thermodynamic cycles. An important thermodynamic cycle is organic Rankine cycle (ORC) due to its high efficiency compared with other traditional Rankine cycle and also for the small size of the thermal generator that use ORC. ORC thermodynamic cycle keeps its high efficiency even for a large variation domain of the thermal fluid temperature [9, 10]. Worldwide, several experimental ORC equipment of small electric power were realized: 0.5 kW [11]; 1 kW [12–14] or 3 kW [15–17].

The mechanical power produced by a ORC thermal machine drives a synchronous electrical generator that will be main component of the smart-grid, playing a master role for the electrical quantities.

Real solutions have led to mathematical relationships that have been implemented in simulation models. The thermal-mechanical-electrical assembly was realized in a simulation with variation in maximum range of input values for geothermal water. The research of the authors could be used to design low power geothermal electric generators, used as main power generators for smart grids in isolated small communities that dispose of geothermal water resources [10]. With the help of the simulation results, one can also estimate the financial costs of a proposed system, due to the fact that the investment amortization lasts long periods of time. Another important contribution is the fact that the authors gave a special attention to the generalization of electrical energy solutions with synchronous motors and models of ORC systems.

2. MODEL OF THE GEOTHERMAL ELECTRIC POWER GENERATOR

The equipment operating under the organic Rankine cycle (ORC) is converting the heat into work and then into electricity. The working principle of this equipment is similar with the classic steam Rankine cycle (SRC) but water as thermal agent is replaced by an organic substance capable to evaporate at much lower temperatures, such as refrigerants. In this study the working agent is R245fa, recommended for the heat source temperatures in the range (80–120) °C [18, 19].

The heat source of this equipment is usually represented by geothermal energy, solar energy or waste heat from industrial or other processes. In this study the heat source is considered the geothermal energy. The interaction between the ORC equipment with the hot and cold sources is presented in Fig. 1.

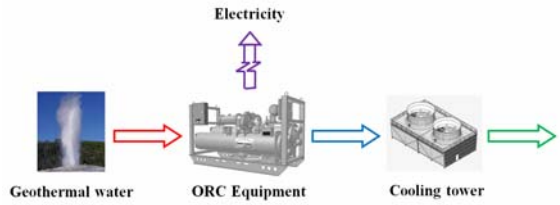

Fig. 1 – The interaction between thee ORC equipment and the heat sources.

The heat is partially transformed into electricity and partially evacuated into the environment by the equipment with the principle scheme presented in Fig. 2.

The low pressure vapors (2) are condensed by thermal power extraction (P_c) in the condenser (C). At the outlet of this process results low pressure liquid (3) that is compressed by the pump (P) by absorption of the mechanical compression power (P_c) and the high pressure liquid (4) is feeding the evaporator closing the working cycle. The compression power is negligible by comparison with all the other involved mechanical and thermal powers.

[1] University of Oradea, str. Universitatii, nr. 1, code 410087, Oradea, Romania, E-mail:oneamtu@uoradea.ro
[2] Technical University of Cluj-Napoca, str. Memorandumului, nr. 28, code 400114, Cluj-Napoca, Romania

The working process of the ORC equipment is presented in the temperature-entropy (*T*–*s*) diagram of R245fa, in Fig. 3.

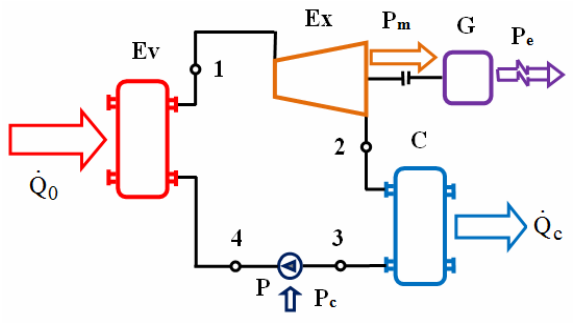

Fig. 2 – The principle scheme of the geothermal ORC system:

Ev – evaporator;
Ex – expander (or turbine);
G – electric generator;
C – condenser;
P – pump;
$\dot{Q}_0$ – thermal power of the heat source;
Pm – mechanical power;
Pe – electrical power;
$\dot{Q}_c$ – thermal power evacuated in the environment;
Pc – mechanical compression power of the pump;
1 – high pressure vapors;
2 – low pressure vapors;
3 – low pressure liquid;
4 – high pressure liquid.

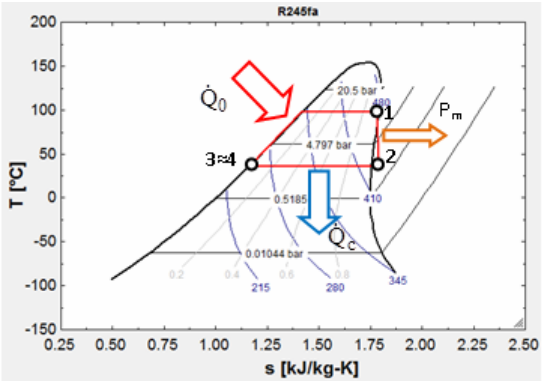

Fig. 3 – the ORC cycle in the T-s diagram of R245fa.

The diagram is provided by the Engineering Equation Solver (EES) software.

The thermal calculation of the ORC cycle was realized with the EES software, following the procedure presented in [9, 20].

3. ORC SIMULATION WITH TRANSFER OF THERMAL POWER IN ELECTRIC POWER

The model of the geothermal electric power generator is based on (1) with mechanical power [9–21]:

$$P(t) = \dot{Q}_0(t) / a(t), \tag{1}$$

where

$$a(t) = 0.0033 \cdot t_h^2(t) - 0.8316 \cdot t_h(t) + 61.973 \tag{2}$$

and t_h is the variable temperature of the geothermal water for the working fluid R245fa.

In the block diagram presented in Fig. 4 the "P" block implements expression (1) of the mechanical power for the case when the input variables [2] come from the INPUT functions generator.

According to Fig. 5, the real values for $\dot{Q}_0(t)$ vary between 30–75 kW and $t_h(t)$ is the geothermal water temperature with variations between 93–120 oC, and are introduced into the simulation by means of the predefined function generator, properly created for correlation with the real ones. Time may be as long as possible, but for experimental tracking through simulation a relatively short time is chosen, when inputs vary over the range of all possible values.

All input and output quantities are obtained with the blocks: "OUT P Q" and "OUT P Q m th" (see Fig. 4). In the block diagram presented in Fig. 4, a power generator was connected to the thermoelectric generator via a block P–P1, used to put in evidence the efficiency of the mechanical conversion:

$$\eta = \frac{P_1}{P} = 0.8. \tag{3}$$

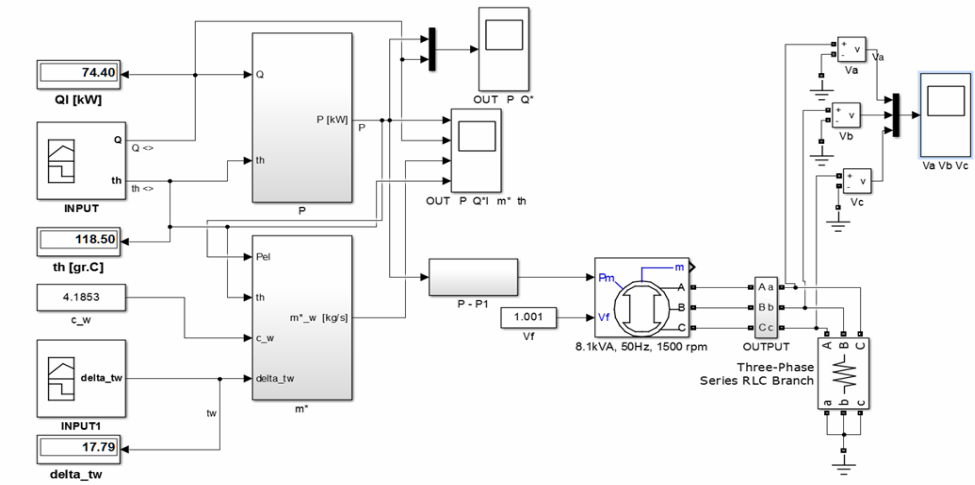

Fig. 4 – Block diagram of a geothermal electric power generator based on organic Rankine cycle.

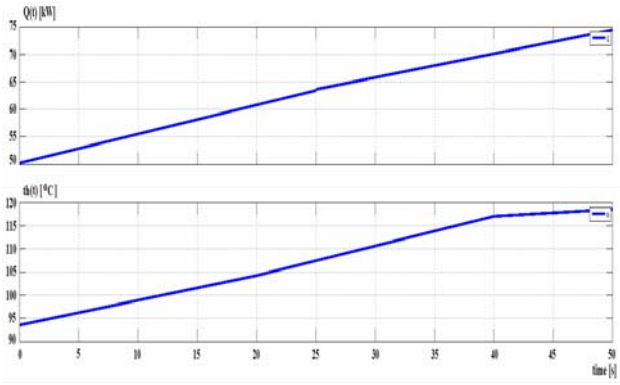

Fig. 5 – Thermal power $\dot{Q}_0(t)$ and temperature $t_h(t)$ for geothermal water as functions of time.

In Fig. 5 is presented the simulation results when the authors imposed a temperature variation between 93 and maximum 120 °C for a period of 50 s. During this variation, the thermal power $\dot{Q}_0(t)$ increases from 50 to 75 kW.

Instead of the required thermal power $\dot{Q}_0(t)$ for geothermal water (see Fig. 4), it can be used flow rate $\dot{m}_w$ [kg/s]:

$$\dot{Q}_0(t) = \dot{m}_w(t) \cdot c_w \cdot \Delta t_w, \tag{4}$$

where the notations are: c_w = 4.1863 kJ/kgK and Δt_w [°C] is the variation of the hot water temperature, usually Δt_w = = (15…20)°C.

The flow rate $\dot{m}_w$ shown in Fig. 6 can be expressed with the next relation:

$$\dot{m}_w(t) = \frac{a(t)}{c_w \cdot \Delta t_w} \cdot P(t). \tag{5}$$

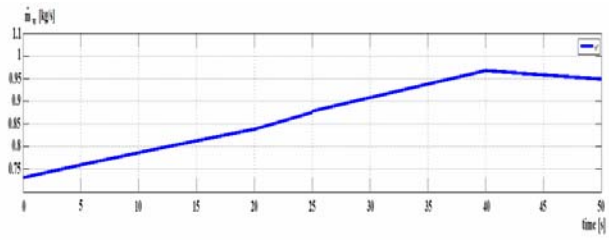

Fig. 6 – The flow rate in dynamic evolution.

In Fig. 6 one can see that the flow rate $\dot{m}_w$ of the thermal agent takes values between 0.7 and 0.98 kg/s for the same simulation conditions mentioned for Fig. 5. The simulations results depicted in Fig. 5 and Fig. 6 give a good evaluation for the designers not only on the quantity of the involved thermal power but also on the quantity of the thermal agent that must be assured during the conversion process.

4. ELECTRIC POWER GENERATOR STAGE

The power generator is implemented for the simulation with a standard three-phase synchronous motor used as a power sine wave generator. In order to evaluate the quantity of the produced energy, a three-phase resistive load has been connected to the generator. In Fig. 7 is shown a dynamic evolution for input geothermal power.

Electrical quantities are viewed from the stator point of view $\dot{Q}_0(t)$ and output electric power $P_{el}(t)$. The output power variation it is between P_{el} = 3÷8kW, when the thermal power variation it is between $\dot{Q}_0$ = 50÷75kW.

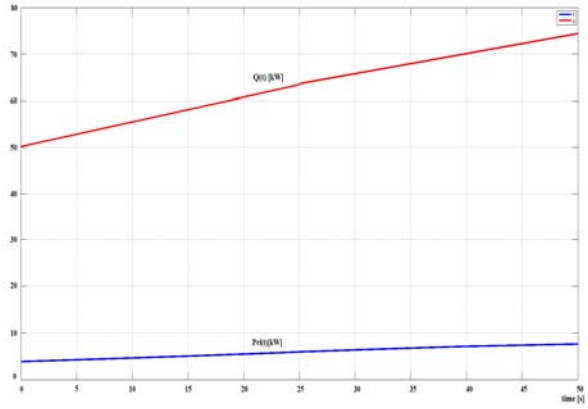

Fig. 7 – Geothermal power $\dot{Q}_0(t)$ and electrical power $P_{el}(t)$.

Synchronous motor [22, 23] operate in generator mode, from the thermo-generator presented in Fig. 4. Dynamical model works in simulation for the classical [24, 25] rotor reference frame (q–d frame).

Electro-mechanical power P_m is input and with internal constructive parameters of the synchronous machine it is realizing the components on the axis of the rotating orthogonal reference frame:

$$P_1 = P_m = \frac{3}{2}\omega_r(\lambda_d i_q - \lambda_q i_d), \tag{6}$$

where: ω_r rotor angular speed; λ is the flux linkage in the q or d axe of the qd0 reference frame; i is the current flowing out of generator.

The inverse transformation matrix from qd0 reference frame in to abc0 three-phase system is:

$$\left[T_{qd0}(\theta)\right]^{-1} = \begin{bmatrix} \cos\theta & \sin\theta & 1 \\ \cos(\theta - \frac{2\pi}{3}) & \sin(\theta - \frac{2\pi}{3}) & 1 \\ \cos(\theta + \frac{2\pi}{3}) & \sin(\theta + \frac{2\pi}{3}) & 1 \end{bmatrix} \tag{7}$$

The values of currents and voltages of the three-phase system are:

$$\begin{bmatrix} i_a \\ i_b \\ i_c \end{bmatrix} = \left[T_{qd0}(\theta)\right]^1 \begin{bmatrix} i_q \\ i_d \\ i_0 \end{bmatrix} \tag{8}$$

$$\begin{bmatrix} v_a \\ v_b \\ i_{vc} \end{bmatrix} = \left[T_{qd0}(\theta)\right]^{-1} \begin{bmatrix} v_q \\ v_d \\ v_0 \end{bmatrix}. \tag{9}$$

It is required by convention for the three-phase symmetrical system:

$$v_0 = \frac{1}{3}(v_a + v_b + v_c) = 0 \tag{10}$$

$$i_0 = \frac{1}{3}(i_a + i_b + i_c) = 0 \tag{11}$$

When there are balanced conditions:

$$v_a = V_m \sin \omega_S t \tag{12}$$

$$v_b = V_m \sin(\omega_S t - \frac{2\pi}{3}) \tag{13}$$

$$v_b = V_m \sin(\omega_S t + \frac{2\pi}{3}) \tag{14}$$

Peak nominal line to neutral voltage is:

$$V_m = (\sqrt{2}/\sqrt{3}) V_{RMS} \tag{15}$$

where $V_{RMS} = 400$ V is fixed in parameters setup.

$$i_a = I_m \sin \omega_S t \tag{16}$$

$$i_b = I_m \sin(\omega_S t - \frac{2\pi}{3}) \tag{17}$$

$$i_e = I_m \sin(\omega_S t + \frac{2\pi}{3}) \tag{18}$$

The peak nominal current is:

$$I_m = (\sqrt{2}/\sqrt{3})(P_{el}/V_{RMS}). \tag{19}$$

The voltages on the three-phases v_a, v_b, v_c, from Fig. 4 are obtained from the OUTPUT block, placed between the generator and the load is used for dynamic measurements. The internal structure of the dynamic measurement OUTPUT block is shown in Fig. 8.

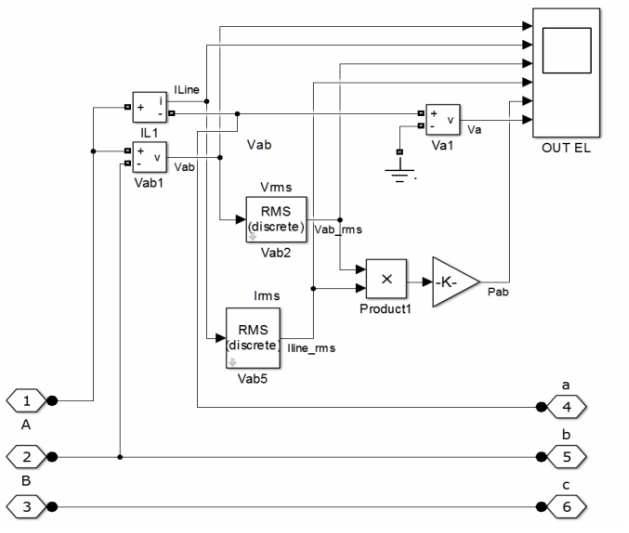

Fig. 8 – The internal structure of the OUTPUT block.

With dedicated blocks, dynamic values for voltages and currents are measured, both instantaneous values and RMS values. The simulation results of the output variables can be seen in Fig. 9.

The stationary electrical power at $P_{el} = 4$ kW is sufficient for the maximum load of an isolated small community.

The outputs voltages on the three-phases power generator are presented in Fig. 10, when is used simulation block-diagram from Fig. 4, with the v_a, v_b, v_c oscilloscope.

There is a stabilization of the waveforms for the three-phase symmetric generator system after a time of 0.3 seconds, when the electrical load is resistive.

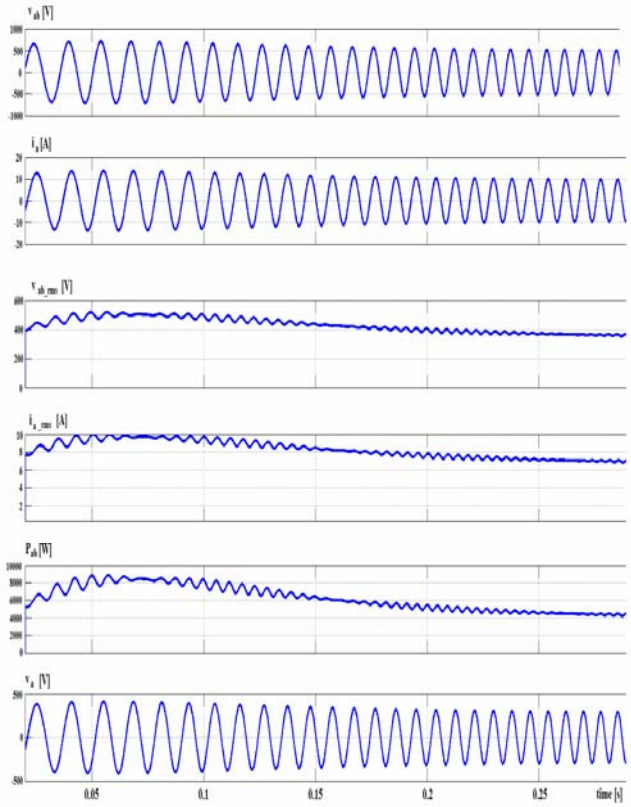

Fig. 9 – Outputs values for power generator.

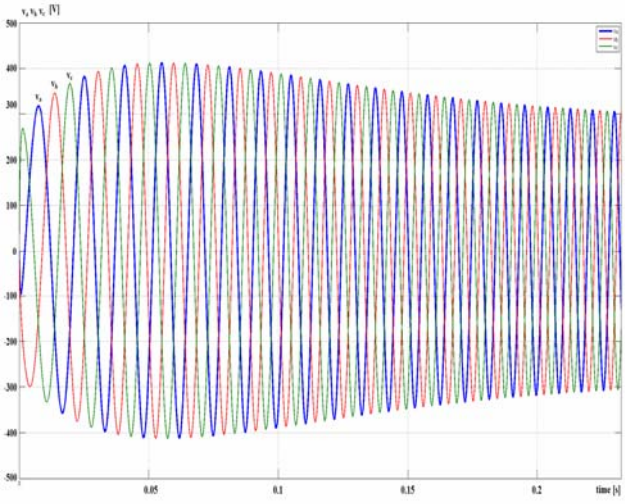

Fig. 10 – The outputs voltages on the three-phases power generator.

5. CONCLUSIONS

The geothermal electric power generator is based analytically and it is modeled for real modules.

Mathematical expressions for ORC are determined experimentally and are entered in functional blocks in the simulation, which are substitute for the real model. Input data are constant or continuous functions whose variation is within the maximum range accepted by the real installation. The synchronous generator introduced in the simulation is taken from a real model with all the constructive parameters included.

The modeling system was partially validated, within the limits of some values in both the thermal-mechanical and mechanical-electrical conversion. The simulation across the range of variation possible provides complete design information. Various thermal sources can be identified, but the purpose of the work was directed to the geothermal water available to the medium thermal power.

For a geothermal water source, with the maximum limits of the temperature variation comprised between 93 ^{o}C and 120 ^{o}C, the authors obtained a thermo – mechanical – electric conversion with an electric power of 4 kW according with the maximal requirements required in the research project carried on by the authors.

ACKNOWLEDGEMENTS

This paper is supported through the programme "Parteneriate in domenii prioritare – PN II", by MEN – UEFISCDI, Project no. 53/01.07.2014.

Received on September 26, 2017

REFERENCES

1. D. Petreus, R. Etz, T. Patarau, C. Orian, *Microgrid concept based on distributed renewable generators for a greenhouse*, Acta Technica Napocensis Electronics and Telecommunications, **56**, *2*, pp. 31–36 (2015).
2. M.O. Neamtu, N.D. Trip, *An Photovoltaic System Tester with Three-Phase Off-Grid Supply Simulation testing with real-equivalent parameters or photovoltaic panels and electronic converter*, 22nd International Symposium for Design and Technology in Electronic Packaging (SIITME), 2016, pp. 191–194.
3. S. Tamalouzt, K. Ididarene, T. Rekioua, R. Abdessemed, *Direct Torque Control of Wind Turbine Driven Doubly Fed Induction Generator*, Rev. Roum. Sci. Techn.– Électrotechn. et Énerg., **61**, *3*, pp. 244–249 (2016).
4. M.O. Neamtu, M.I. Gordan, N.D. Trip, *A geothermal thermo-electric energy converter for charging lithium-ion battery*, Fundamentals of Electrical Engineering (ISFEE), 2014 International Symposium (IEEE).
5. Eniko Lazar, T. Patarau, R. Etz, D. Petreus, *Sizing Photovoltaic-Geothermal Smart Microgrid with Battery Storage Interface*, 38th International Spring Seminar on Electronics Technology, Eger, Hungary, May, 6–10, 2015.
6. M. Cârdu, I. Ionel, C. Ungureanu, *Combined nuclear and conventional plant, operating on hydrogen, according to Rankine cycle***,** Rev. Roum. Sci. Techn. – Électrotechn. et Énerg., **52**, *1*, pp. 105–119 (2007).
7. I.M. Gordan, D.M. Purcaru, C. Vancea, *Contributions to Optimize the Operation of a Thermoelectric Conversion Equipment*, Journal of Electrical and Electronics Engineering, **7**, *1* , pp. 53–56 (2014).
8. I. Felea, C. Panea, G. Bendea, *Stochastic evaluation of the reliability of the geothermal energy exploitation systems*, Rev. Roum. Sci. Techn. – Électrotechn. et Énerg., **59**, *2*, pp. 141–151 (2014).
9. P.V. Unguresan, D. Petreus, M.C. Balan., *Model for the behaviour of low temperature and small size ORC equipment*, Buletinul Institutului Politehnic din Iasi, **LXI** (LXV), *2*, Secția Construcții de Mașini, pp. 73–82 (2015).
10. R. Etz, D. Petreus, T. Patarau, Eniko Lazar, *An islanded renewable energy microgrid emulator for geothermal, biogas, photovoltaic and lead acid battery storage*, 26th IEEE International Symposium on Industrial Electronics (ISIE), Edinburgh, Scotland, UK, 19–21 June 2017.
11. M. Jradi, L. Jinxing, H. Liu, S. Riffat, *Micro-scale ORC-based combined heat and power system using a novel scroll expander*, International Journal of Low-Carbon Technologies, *9*, pp. 9–99 (2014).
12. V. Lemort, S. Declaye, S. Quoilin, *Experimental characterization of a hermetic scroll expander for use in a micro-scale Rankine cycle*, Proceedings of the Institution of Mechanical Engineer: Part A: Journal of Power and Energy, 2011, pp. 126–136.
13. D. Meyer, C. Wong, F. Engel, S. Krumdieck, *Design and Build of a 1 Kilowatt Organic Rankine Cycle Power Generator*, Proceedings of 35th New Zealand Geothermal Workshop, Rotura, New Zeeland, 17–20 November, 2013.
14. S. Quoilin, V. Lemort, J. Lebrun, *Experimental study and modeling of an Organic Rankine Cycle using scroll expander*, Applied Energy, **87**, pp. 1260–1268 (2010).
15. M. Orosz, A. Mueller, S. Quoilin, *Small Scale Solar ORC system for distributed power*, Proc. of the Solar Paces Conference, 2009.
16. E. Georges, S. Declaye, O. Dumont, S. Quoilin, V. Lemort, *Design of a small-scale organic Rankine cycle engine used in a solar power plant*, International Journal of Low-Carbon Technologies, **8**, pp. 134–141 (2013).
17. R. Zanelli, D. Favrat, *Experimental Investigation of a Hermetic Scroll Expander-Generator*, International Compressor Engineering Conference, Paper 1021, 1994.
18. V. Lemort, L. Guillaume, A. Legros, S. Declaye, S. Quoilin, *A comparison of piston, screw and scroll expanders for small scale Rankine cycle systems*, Proceedings of the 3rd International Conference on Microgeneration and Related Technologies, 2013.
19. S. Quoilin, M. VanDenBroek, S. Declaye, P. Dewallef, V. Lemort, *Techno-economic survey of Organic Rankine Cycle (ORC) systems*, Renewable and Sustainable Energy Reviews, **22**, pp. 168–186 (2013).
20. P.V. Unguresan, D. Petreus, A.G. Pocola., M.C. Balan, *Potential of solar ORC and PV systems to provide electricity under Romanian climatic conditions*, Energy Procedia, **85**, pp. 584–593 (2016).
21. M. Angelino, M. Gaia, E. Macchi, *A review of Italian activity in the field of Organic Rankine Cycles*, Proceedings of the International VDI-Seminar, Zürich, 10–12 September, 1984.
22. A. Campeanu, R. Munteanu, V. Iancu, *Abaut Dynamic Stability of High Power Synchronous Machine. A Review*, Rev. Roum. Sci. Techn. – Électrotechn. et Énerg., **62**, *1*, pp. 8–13 (2017).
23. D. Ilina, *Estimation of the Numerical Model Parameters for the Synchronous Machine Using Tests at Standstill,* Rev. Roum. Sci. Techn.– Électrotechn. et Énerg., **61**, *1*, pp. 13–17 (2016).
24. P. Kundur, *Power System Stability and Control*, McGraw-Hill, 1994.
25. C.M. Ong., Dynamic Simulation of Electric machinery, Prentice Hall PTR, 1998.